Atmos. Chem. Phys. Discuss., 11, 19683–19727, 2011
www.atmos-chem-phys-discuss.net/11/19683/2011/
doi:10.5194/acpd-11-19683-2011

Atmospheric Chemistry and Physics Discussions

On aerosol hygroscopicity, cloud condensation nuclei (CCN) spectra and critical supersaturation measured at two remote islands of Korea between 2006 and 2009

J. H. Kim[1], S. S. Yum[1], S. Shim[2], S.-C. Yoon[3], J. G. Hudson[4], J. Park[5], and S.-J. Lee[5]

[1]Department of Atmospheric Sciences, Yonsei University, Seoul, Korea
[2]National Institute of Meteorological Research, Seoul, Korea
[3]School of Earth and Environmental Sciences, Seoul National University, Seoul, Korea
[4]Division of Atmospheric Sciences, Desert Research Institute, Reno, Nevada, USA
[5]National Institute of Environmental Research, Incheon, Korea

Received: 2 June 2011 – Accepted: 22 June 2011 – Published: 11 July 2011

Correspondence to: S. S. Yum (ssyum@yonsei.ac.kr)

Published by Copernicus Publications on behalf of the European Geosciences Union.

Abstract

Aerosol size distribution, total concentration (i.e., condensation nuclei (CN) concentration, N_{CN}), cloud condensation nuclei (CCN) concentration (N_{CCN}), hygroscopicity at ~90 % relative humidity (RH) were measured at a background monitoring site at Gosan, Jeju Island, south of the Korea Peninsula in August 2006, April to May 2007 and August to October 2008. Similar measurement took place in August 2009 at another background site (Baengnyeongdo Comprehensive Monitoring Observatory, BCMO) on the island of Baengnyeongdo, off the west coast of the Korean Peninsula. Both islands were found to be influenced by continental sources regardless of season and year. Average values for all of the measured N_{CCN} at 0.2, 0.6 and 1.0 % supersaturations (S), N_{CN}, and geometric mean diameter (D_g) from both islands were in the range of 1043–3051 cm^{-3}, 2076–4360 cm^{-3}, 2713–4694 cm^{-3}, 3890–5117 cm^{-3} and 81–98 nm, respectively. Although the differences in D_g and N_{CN} were small between Gosan and BCMO, N_{CCN} at various S was much higher at the latter, which is closer to China.

Most of the aerosols were internally mixed and no notable differences in hygroscopicity were found between the days of strong pollution influence and the non-pollution days for both islands. During the 2008 and 2009 campaigns, critical supersaturation for cloud nucleation (S_c) for selected particle sizes was measured. Particles of 100 nm diameters had mean S_c of 0.19 ± 0.02 % during 2008 and those of 81 and 110 nm diameters had mean S_c of 0.26 ± 0.07 % and 0.17 ± 0.04 %, respectively, during 2009. Hygroscopicity parameters estimated from the measured S_c were mostly higher than the ones from the measured hygroscopic growth at ~90 % RH.

For the 2008 campaign, N_{CCN} at 0.2, 0.6 and 1.0 % S were predicted based on the measured dry particle size distribution and various ways of representing aerosol hygroscopicity. The best closure was obtained when temporally varying and size-resolved hygroscopicity information from HTDMA was used, for which the average relative deviations from the measured values were 19 % for 1.0 % S and 28 % for 0.2 % S.

ACPD
11, 19683–19727, 2011

Prescribing a constant hygroscopicity parameter suggested in literature ($\kappa = 0.3$) for all sizes and time resulted in the average relative deviations, 25–40 %. When constant hygroscopicity was assumed, the relative deviation tended to increase with decreasing N_{CCN}, which was accompanied by increase of sub-100 nm fraction. These results suggest that hygroscopicity information for aerosols of diameters smaller than 100 nm is crucial for more accurate prediction of N_{CCN}.

1 Introduction

The necessity to gain sufficient understanding of cloud condensation nuclei (CCN) has been increasing within the scientific community due to the realization that anthropogenic emissions of CCN are imposing the greatest uncertainty on climate change prediction (IPCC, 2007; Schwartz et al., 2010). The CCN activity is controlled by the size of aerosols, the supersaturation (S) of the environment surrounding the aerosols, the dissolution behavior of the aerosol within the droplet and its surface tension (Pruppacher and Klett, 1997).

With the development and the dissemination of techniques such as differential mobility analyzer (DMA) (Knutson and Whitby, 1975), measurements of ambient aerosol number size distribution have increased in the last few decades, although the global coverage of such data are yet still far from sufficient (Kumala et al., 2004).

Direct measurement of CCN is much scarcer due to the difficulty of the measurements and the lack of instruments. Measuring the hygroscopicity of aerosols under sub-saturated conditions of water vapor was suggested as a tool for estimating CCN activity of aerosols. In these studies measured hygroscopicity was used to predict the critical supersaturation (S_c) of particles, which is the threshold S above which the thermodynamic equilibrium between the aerosols and the surrounding vapor collapses and the vapor continuously condenses onto the aerosol without requiring higher S. Recent development of a single parameter κ that provides a theoretical link between hygroscopicity at sub-saturated condition to cloud activation (Petters and Kreidenweis,

ACPD
11, 19683–19727, 2011

2007) with minimal assumption made such an approach more feasible. However, the hygroscopicity data for ambient aerosols are scarce (Swietlicki et al., 2008) and only a few studies are available for ambient S_c measurement (Dusek et al., 2006; Hudson and Da, 1996; Hudson, 2007).

For most of present day climate models, information on CCN number concentration (N_{CCN}) at certain S is needed. To fulfill this requirement, many attempts have been made to retrieve N_{CCN} from aerosol hygroscopicity and size measurements at various regions including subarctic (Kammermann et al., 2010), Amazon rainforest (Gunthe et al., 2009; Vestin et al., 2007; Zhou et al., 2002), coastal locations (Dusek et al., 2003; Kuwata et al., 2008), rural continental sites (Dusek et al., 2006; Gasparini et al., 2006) and large cities (Lance et al., 2009; Rose et al., 2010). Several authors have raised attention on the effect of aerosol mixing state on N_{CCN} (Ervens et al., 2010; Wang et al., 2010; Wex et al., 2010).

In this study, we try to characterize hygroscopicity as well as S_c of aerosols measured in Asian continental outflow. Although various studies have already investigated CCN and hygroscopic properties of the aerosols in this region (e.g., Adhikari et al., 2005; Eichler et al., 2008; Kuwata et al., 2008; Kuwata and Kondo, 2008; Massling et al., 2007, 2009; Matsumoto et al., 1997; Mochida et al., 2010; Rose et al., 2010; Wiedensohler et al., 2009; Yum et al., 2005, 2007), the scope of their spatial and temporal coverage was very limited despite the fact that the region has been under heavy industrial development for the last several decades. Here we present the results from four different field campaigns that took place at the western coastal sites on two remote islands around the Korean Peninsula (Fig. 1) from 2006 to 2009.

ACPD
11, 19683–19727, 2011

2 Measurement and campaign description

2.1 Gosan, Jeju Island

The two measurement shelters (about 10 m apart) located at the top of a cliff at Gosan (33.2° N, 126.1° E, 70 m a.s.l., Fig. 1) were used. Since local sources near the site are limited, this site has served as a supersite for several international campaigns, including ACE-ASIA (Hubert et al., 2003), ABC-EAREX2005 (Nakajima et al., 2007), Pacific Dust Experiment (PACDEX) (Stith et al., 2009) and Cheju ABC Plume-Asian Monsoon Experiment (CAPMEX) (Ramana et al., 2010). The measurements took place at three different periods: 15 August–1 September 2006 (hereafter denoted as Gosan 2006); 14 April–16 May 2007 (Gosan 2007); 1 August–11 October 2008 (Gosan 2008).

A TSI condensation particle counter (CPC) 3010 and a TSI SMPS 3936L10 were used to measure the total number concentration of aerosols (i.e., condensation nuclei (CN) concentration, N_{CN}) having diameter 10–300 nm. Sample air for the SMPS was not dried except during 2008. For CCN number concentration (N_{CCN}) measurement, the Desert Research Institute Instantaneous CCN Spectrometers (CCNS) (Hudson, 1989) were used in Gosan 2006 and a Droplet Measurement Technologies (DMT) CCN counter (CCNC) (Roberts and Nenes, 2005) was used in all other campaigns. The two CCN instruments were calibrated with monodisperse ammonium sulfate or sodium chloride particles and the Köhler model denoted as analytical approximation 1 (AA1) by Rose et al. (2008) was used to obtain the S_c of these particles.

Hygroscopic growth factors for dry aerosol between 50 and 250 nm were measured by typical humidified tandem differential mobility analyzer (HTDMA). RH was measured by 3 capacity-type RH sensors either from Vaisala (model HMM22d, uncertainty of ±2 % RH) or Testo (model 06369735 and model 06369740, uncertainty of ±2 % RH) at the exits of the first DMA, nafion humidifier and the sheath air of the second DMA. The RH sensors were calibrated by the local distributors of the instruments before each campaign. The hygroscopicity measurement was performed only for several hours in each day during Gosan 2006 while continuous measurements were done for Gosan 2007 and Gosan 2008.

ACPD
11, 19683–19727, 2011

The mass concentration for particles smaller than 10 µm (PM_{10}) and 2.5 µm ($PM_{2.5}$) and gas concentrations of sulfur dioxide (SO_2), carbon monoxide (CO), ozone (O_3), nitrogen dioxide (NO_2) were measured with Met One BAM1020, Met One FH-62, TEI 43C-TL, TEI 48C, TEI 49C and TEI 42CTL, respectively, at the second shelter maintained by NIER.

The S_c of monodisperse particles of selected sizes were measured along with N_{CCN} during Gosan 2008 by the configuration shown in Fig. 2. The sample air was led to the dryer, aerosol neutralizer and DMA at the upper branch located in between the two 3-way valves before reaching the CPC and CCNC. First, the aerosols with dry diameter (D_{dry}) of 50 or 100 nm were selected by the DMA. The resulting size-segregated N_{CCN} to N_{CN} ratios were plotted against the 12 S values between 0.07 % and 1.5 % S (Fig. 3). The S_c was then identified as the S at which the height of the fitted sigmoid curve was the half of the maximum height. In order to take multiply charged aerosols into account, which would create a small hill at lower S, sigmoid curve was allowed to have non-zero y-intercept.

2.2 BCMO, Baengnyeongdo

Similar measurement took place at Baengnyeongdo Comprehensive Monitoring Observatory (BCMO) (about 150 m a.s.l.; 38.0° N, 124.6° E) in the island of Baengnyeongdo (Fig. 1) during 5–30 August 2009 (BCMO 2009). Local sources near the site are also very limited and BCMO serves as a background air quality monitoring station. The TSI CPC 3010, HTDMA and CCNC configuration in Fig. 2 were again used. Aerosol size distribution was measured only during the last three days by a TSI SMPS 3936L10. The CCNC was calibrated by a similar process as stated above.

PM_{10}, $PM_{2.5}$, SO_2, CO, O_3, NO_2 were also measured with Thermo 1400A, Thermo 1405, Teledyne 100A, Teledyne 300EU, Teledyne 400E and Teledyne 200AU, respectively.

ACPD
11, 19683–19727, 2011

3 Results

3.1 PM and gaseous species concentrations

Based on the daily average PM_{10}, $PM_{2.5}$, SO_2, O_3, CO, NO_2 (or NO_y for BCMO 2009) concentration data, days with significant pollution were identified for each campaign. Such days were 17–18 and 28 August 2006; 26–27 April and 7–8 May 2007; 18–22 August and 30 September–11 October 2008; and 13–16 August 2009. Relatively higher concentrations of SO_2 and O_3 were general characteristics of the pollution periods and high $PM_{2.5}$ and PM_{10} concentrations were also found in all pollution periods except for the later pollution period in 2008. It should be noted that the distinction between the pollution days and non-pollution days is relative. For example, according to Flower et al. (2010)'s classification of pollution periods based on optical and chemical composition measurement of aerosols at the Gosan site, 74 % of the days in August and September, 2008 were designated as pollution days. The pollution period classified in this study constitutes a minor fraction of their pollution period.

Figure 4 shows the average values for each classification. Gosan 2007 showed generally high concentrations in all species and especially for the pollution period, it had the highest concentrations in all species. Meanwhile, Gosan 2006 showed the lowest PM_{10} and O_3 concentrations among the four campaigns but CO concentrations for all data and non-pollution days were the highest. The SO_2 concentration during Gosan 2008 was significantly lower than during the other campaigns, but its CO concentration is comparable to those in the other campaigns. BCMO 2009 had the lower $PM_{2.5}$ and NO_2 (which is a subset of NO_y) concentrations than those during the campaigns at Gosan, but its SO_2 concentration was the highest among all four campaigns except for Gosan 2007 pollution days. Therefore, no campaign had all six species low. These results indicate that the two sites were exposed to continental sources to some extent, even for the non-pollution period within each campaign.

The CO concentrations measured in our campaigns were mostly above 0.3 ppm, which is much greater than the values measured in nonurban tropospheric air,

ACPD
11, 19683–19727, 2011

0.07–0.2 ppm (Hobbs, 2000). Based on the 13-year long-term measurement, Kaneyasu (2010) reported that continental influence was evident at Chichi-jima Island (27.07° N, 142.22° E) from late autumn to spring, which lies in the Northwestern Pacific 1800 km to the east of Chinese coastline. Even during the rest of the seasons, their black carbon concentration was still higher than other background sites around the world, suggesting that the region still might not be completely free from continental influence. Compared to Chichi-jima Island, both islands in this study are located at a distance much closer to continental sources (< 100 km from the Korean Peninsula and < 500 km from China). Based on the ship measurement during the cruise from a port in Jeju Island to Shanghai, Kim et al. (2009a) found that the instantaneous minimum N_{CN} in East China Sea (1025 cm^{-3}) was still higher than the average N_{CN} measured at other background marine regions by a factor of two to five (Bates et al., 2002; Covert et al., 1996; Hoppel et al., 1990; Yum and Hudson, 2001). These previous studies also suggest that the two islands were under constant continental influence although its source could be different. Since the contribution of sea salt is known to take only a minor portion in PM_{10} or $PM_{2.5}$ at the two islands (Lee et al., 2007; Kim et al., 2009b), high PM_{10} concentration can be considered as originated from continental sources.

3.2 Aerosol size distributions and CCN spectra

Some important statistics of the aerosol physical properties and N_{CCN} measured during each campaign are shown in Table 1 and the average CCN spectrum for each campaign is shown in Fig. 5. The N_{CN} from all four campaigns are comparable to that measured over the seas around the Korean Peninsula (Kim et al., 2009a), indicating that the two islands represent the maritime environment in the region. However, the same values are also higher than those from a pollution event at Gosan during 2001 (Kim et al., 2005), indicating that the two islands are constantly under continental influence.

The average N_{CN} in BCMO 2009 was the highest among the four campaigns. This is consistent with the previous study by Kim et al. (2009a) who showed that the N_{CN} over

ACPD
11, 19683–19727, 2011

the Yellow Sea, where Baengnyeongdo lies, was higher than those over the South Sea of Korea and East China Sea, which is surrounding Jeju Island. At BCMO, not only N_{CN} but also N_{CCN} was higher than at Gosan during the other campaigns for all measured $S \geq 0.1$ % (Fig. 5). On the other hand, the lowest N_{CCN} was measured during Gosan 2008. The smaller D_g during Gosan 2008 than during the other campaigns is thought to be due to the effect of drying the SMPS sample air only in this campaign.

Time series of N_{CN}, N_{CCN} and D_g are shown in Fig. 6. During the pollution days, N_{CN} and N_{CCN} tended to be at local maximum but comparably high concentrations were also frequently found during some non-pollution days. The D_g values were generally larger during the pollution days, mostly larger than 100 nm, implying that they had gone through aging processes accompanied by condensation since their fresh emission.

3.3 Hygroscopic growth factors under 90 % RH

For this section, the growth factor (GF, defined as the ratio between the wet diameter and D_{dry}) values measured at various RH were converted to GF at 90 % RH (GF90) by the method illustrated in Swietlicki et al. (1999) to facilitate comparison across different campaigns. Converted GF90 values were then classified into four categories; "nearly hydrophobic" for GF90 smaller than 1.15, "less hygroscopic" for GF90 between 1.15 and 1.55, "more hygroscopic" for GF90 between 1.55 and 1.85 (similar to GF90 of ammonium sulfate) and "very hygroscopic" for GF90 larger than 1.85. This classification is similar to that done by Massling et al. (2007) except they denoted the class with the largest GF90 as "sea salt." Selected D_{dry} sizes varied in each campaign: 50, 100, 150 and 200 nm for Gosan 2006; 100, 150, 200 and 250 nm for Gosan 2007; 50, 100, 150, 200 and 250 nm for Gosan 2008; 53, 113, 163 and 225 nm for BCMO 2009.

The relative frequency of occurrence, or the cumulative number fraction, of each hygroscopicity class is shown for each campaign and each D_{dry} in Fig. 7. The average GF90 values and number fractions are listed in Table 2. As shown in Fig. 7, most of the GF90 values fell into either less or more hygroscopic class ($1.15 \sim 1.85$). Particles measured during Gosan 2007 and Gosan 2008 tended to show lower hygroscopicity

ACPD
11, 19683–19727, 2011

compared to those measured at Gosan 2006 and BCMO 2009. Overall hygroscopicity was larger during BCMO 2009 than during the other campaigns, which is consistent with the above finding that N_{CCN}/N_{CN} for $S \leq 0.6\,\%$ and SO_2 were the largest during BCMO 2009 among the four campaigns.

As for the mixing state, 82 %, 97 %, 99 % and 98 % of the HTDMA samples measured during Gosan 2006, Gosan 2007, Gosan 2008 and BCMO 2009, respectively, had only a single GF mode, suggesting that the aerosols were mostly internally mixed. During Gosan 2006, Gosan 2007 and Gosan 2008, when there was more than one GF mode within the sample, "nearly hydrophobic" particles were highly likely to be found (more than four out of five). For Gosan 2008, however, more than half of "nearly hydrophobic" particles were found with a single GF mode. During BCMO 2009, "nearly hydrophobic" particles were found only in a small fraction. Even when the sample had more than one GF mode, it consisted only of "less hygroscopic" and "more hygroscopic" modes, suggesting that these particles have gone through aging processes maybe due to high sulfur concentration around the region. The GF90 values during the pollution days were similar to those during the non-pollution days, suggesting that continental sources were constantly affecting the sites even on the days classified as non-pollution days.

When compared to the previous HTDMA measurement during ACE-Asia (Massling et al., 2007), the values during Gosan 2006 in Table 2 are similar to the result for the pollution from Shanghai and dust period measured onboard the NOAA Research Vessel Ronald H. Brown at a location about 400 ~ 600 km east of Gosan, where a minor but significant portion was "nearly hydrophobic" and the most abundant class was "more hygroscopic." Gosan 2007 and Gosan 2008 were unique in that the "less hygroscopic" class was dominant. BCMO 2009 is similar to the case when the pollution had passed over Korea and Japan before reaching the R/V Ronald H. Brown, although the majority of air masses were from Northeastern China during BCMO 2009.

The GF90 values in this study were mostly in the range of 1.4 ~ 1.7, similar to or even higher than the most hygroscopic modes measured in Beijing during the summer 2004 and the winter 2005 (Massling et al., 2009), which is located at the dominant upwind

ACPD
11, 19683–19727, 2011

region. As with the previous discussion, this is another indication that the aerosols reaching the two islands have gone through chemical aging during the transport.

3.4 Critical supersaturation (S_c)

Time variations of the S_c measured during Gosan 2008 and BCMO 2009 are plotted in Fig. 8. Note that the measurement period was much longer during Gosan 2008. As shown in Fig. 8a, some S_c data were missing for 50 nm during Gosan 2008 because the full shape of sigmoid curve as in Fig. 3 could not be constructed. During BCMO 2009, the S_c for the two monodisperse dry particle sizes were relatively larger for periods before 13 August than after 13 August. Such distinction between the periods was also found in the $PM_{2.5}$ and SO_2 data. According to the 72 h back trajectory analysis, all the air masses that reached BCMO before 13 August passed over the Korean Peninsula whereas the air mass after 13 August mostly passed over Northeastern China. Kim et al.(2009b) reported a clear distinction in inorganic compound of submicron particles measured by an Aerodyne aerosol mass spectrometer at BCMO between the back trajectories that passed over the Korean Peninsula and those over the Northeastern China region such as Shandong Peninsula/Bohai Bay. Nitrate was abundant for the former while sulfate was abundant for the latter. The difference in S_c between the two periods cannot be attributed to the difference in nitrate and sulfate concentrations because nitrate can act as good CCN as sulfate (Brechtel and Kreidenweis, 2000) and because the abundant amount of organics for both back trajectories also need to be considered. Different aerosol compositions, however, reveal that aerosol sources were different between the two regions. From a field study during spring 2008, Mochida et al. (2010) reported that aerosols reaching Cape Hedo from China and the Pacific had higher GF, compared to those from Korea and Japan, which may be supportive to our results. On the other hand, no such clear distinction of S_c was found during Gosan 2008.

In Table 3 CCN activity parameters (diameter of particles that can be activated as CCN at a given S (D_{p_act}), critical supersaturation (S_c) or growth factor (GF90)) reported

ACPD
11, 19683–19727, 2011

in previous studies in East Asia are compared with those measured in this study along with the corresponding values of hygroscopicity parameter κ (Petters and Kreidenweis, 2007). Overall, the κ values measured during BCMO 2009 are higher than those measured during Gosan 2008, which is in accordance with the N_{CCN}/N_{CN} and HTDMA data.

Although no previous studies have measured S_c in East Asia, several studies have characterized CCN activity by measuring the D_{p_act} with similar instrument setup as in Fig. 2. Those studies varied D_{dry} and set S fixed ("D_{dry} scan") while in this study instead S was varied ("S scan") and D_{dry} was fixed. Under the assumption that aerosols are all internally mixed and that aerosols have homogeneous hygroscopicity across the whole submicron size range, CCN activity measured from both settings should agree with each other.

Su et al. (2010) quantified the difference between the two methods if aerosol hygroscopicity varies with particle size. They considered a case when κ varied with size as $\kappa = 0.2\left(\frac{D_{Dry}}{20\ nm}\right)^{0.4}$ that causes much larger variation compared to the ones measured in this study. They concluded that the difference between the two methods due to size-dependent hygroscopicity should be relatively minor compared to the instrumental uncertainties. Since the aerosols were mostly internally mixed except for Gosan 2006, as discussed above, it would not be too misleading to compare S_c in this study by "S scan" to the activation diameter obtained in previous studies by "D_{dry} scan" when both measured quantities are converted to κ.

As shown in Table 3, the values of κ obtained at Gosan by HTDMA show a decreasing trend since 2005, and the decrease is more significant for smaller D_{dry}. Seasonal variation is not sufficient to explain such decreasing trend since the campaign in 2005 and Gosan 2007 were both carried out during late spring. Moreover, the measurement days of Gosan 2006 are covered by those of Gosan 2008. Such trend is also found for DMA-CCN data: the κ values measured during 2005 are larger than those measured during Gosan 2008. Although the two DMA-CCN measurements were based on different concepts i.e., "D_{dry} scan" for 2005 and "S scan" for 2008, the difference between

ACPD
11, 19683–19727, 2011

the two sets of κ values are too large to be attributed to methodological difference as discussed above. The reason behind such decreasing trend is left unknown.

When the air mass is coming from Northeast China near Yufa, about 50 km south of Beijing, it usually takes a day or two for the air mass to reach BCMO. When the results from Wiedensohler et al. (2009) is presumed to be representative of Northeast China during August 2009, one can say that the hygroscopicity increased as the air mass advected from Northeast China to BCMO, perhaps due to aging processes during the transport.

4 Discussions

4.1 CCN spectrum parameterization

In Fig. 5 the power law approximations ($N_{CCN} = C \times S^k$) to the measured CCN spectra are also shown as dotted lines for each campaign with the corresponding color. The approximation is based on N_{CCN} for $S \geq 0.2\,\%$ but the lines are extrapolated to the smallest S. The range of $S \geq 0.2\,\%$ was selected for two reasons; the spectra show somewhat linear behavior in this range and many N_{CCN} measurements are made for $S \geq 0.2\,\%$. The parameters (C, k) for the power law approximation for $S \geq 0.2\,\%$ are shown in Table 4.

However, it should be noted that the power law approximation usually holds only for limited range of S, as various previous studies have emphasized (Khain et al., 2000 and references therein). Dusek et al. (2003) have also argued that using a traditional power function was not backed by any physical reason and that its application should be confined only to clean marine CCN spectra. As can be seen in Fig. 5, although the power law approximation had high r^2 values for the linear regression between the measured and parameterized N_{CCN} values for $S \geq 0.2\,\%$ (0.98, 0.96, 0.89 and 0.94 for 2006, 2007, 2008 and 2009 campaign, respectively), they all significantly overestimated N_{CCN} at $S < 0.2\,\%$ and the magnitude of overestimation increased with decreasing S. The

ACPD
11, 19683–19727, 2011

N_{CCN} predicted by the power law approximation at 0.02 % S for Gosan 2006, and at 0.07 % S for Gosan 2008 and BCMO 2009 were 3.9, 3.2 and 4.3 times larger than the measured N_{CCN} at the corresponding S, respectively. For that reason, the parameters C and k that can be obtained by linearly extending the CCN spectra only for the range of $S \leq 0.2$ % in Fig. 5 to 1 % S are also shown in Table 4.

4.2 Comparison of hygroscopic growth and cloud activation

Figure 9 compares the estimated κ values from the S_c measurements of monodisperse particles during Gosan 2008 (50 and 100 nm) and BCMO 2009 (110 nm) with those from the simultaneous HTDMA measurements for the same diameters. The κ (GF) was calculated from the actual GF and RH, not GF90. Most of the κ (S_c) was larger than the simultaneously measured κ (GF) although the difference between the two was much smaller for BCMO 2009. The linear regression slopes were 1.64, 1.67 and 1.01, respectively, for each of the three plots in Fig. 9 and their r^2 values were all below 0.5.

The differences between κ (S_c) and κ (GF) found in most of the samples are beyond the probable instrumentation uncertainty. Petters and Kreidenweis (2008) showed that the presence of sparingly soluble organics within the aerosols which dissolve only at supersaturated condition could contribute to higher κ (S_c), although this may not explain the whole differences. Detailed chemical analysis of aerosols is out of the scope of this study but it was reported that significant organic fraction was consistently found in the submicron particles measured both at Gosan (Lee et al., 2007) and BCMO (Kim et al., 2009b), which may have caused such effect.

4.3 CCN closure study

Since CCN activity of aerosol mostly depends on D_{dry}, hygroscopicity and S, N_{CCN} for a given S can be predicted from aerosol dry size distribution and hygroscopicity data. Recently, Andreae and Rosenfeld (2008; hereafter AR08) put together various hygroscopicity measurements around the world and suggested that $\kappa = 0.3 \pm 0.1$ be used for

ACPD
11, 19683–19727, 2011

global continental aged aerosols in numerical models targeted for understanding the aerosol indirect effects on climate.

As shown in previous sections, it is certain that most of the aerosols measured in this study have continental origin and that they have gone through aging processes during transport. Therefore, the data presented in this work will provide a suitable test bed for hygroscopicity values suggested by AR08. The fact that hygroscopicity was measured with high temporal resolution will also enhance the understanding of how size and temporal variation affect N_{CCN}.

In order to do so, measured N_{CCN} are compared with the values predicted by several different methods where hygroscopicity was uniquely assigned to individual size bins for each method. Since all of these methods require dry size distribution data, CCN closure was performed only for the data obtained during Gosan 2008 because size distribution was not measured at dried state during the other campaigns. All aerosols were assumed to be internally mixed, since 99 % of the samples were internally mixed during Gosan 2008 as shown in the previous section. With the assumption of all particles internally mixed in the same proportions for all sizes, a κ value is assigned to each size bin in dry size distribution data and compared with the minimum κ required for the particles in that size bin to be activated as CCN at a given S. If the assigned κ for that size bin is larger than the minimum κ for activation at the given S, then all of the particles in that size bin are counted as CCN. After carrying out such comparisons and counting cumulatively the concentrations in all size bins that meet the condition, the predicted N_{CCN} is obtained. One thing to note is that κ can vary within each size bin because of composition variations among particles in the same size bin but this was not taken into account in our study.

For the first method, denoted as "Method 1-GF", the measured GF was first converted to the corresponding κ (GF, D_{dry}) and then was averaged on hourly basis for every size bin. Then the 1-h averaged κ (GF, D_{dry}) was linearly interpolated over the size bins with log-uniform interval. For the size bins lying outside the hygroscopicity measurement, the measured κ value of the nearest D_{dry} was used. An example of

ACPD
11, 19683–19727, 2011

such procedure is shown in Fig. 10. The solid line indicates the assigned κ value to each size bin interpolated from κ (GF, D_{dry}). The dashed line denotes the minimum κ required for particles in each size bin to be activated as CCN at 0.6 % S. The simultaneously measured dry aerosol size distribution is also shown. Only the particles in the size bins where the assigned κ values are greater than the minimum κ (colored in grey) is assumed to be activated as CCN and they are cumulatively counted for predicting N_{CCN} at 0.6 % S.

The second method is similar to the first one except that it ignores the size-resolving information. This is to see the effect of size-resolved hygroscopicity on N_{CCN}. The average κ (GF) from the two smallest diameters for each hour was applied to all size bins measured during that hour. The reason for choosing the two smallest diameters for representing the hygroscopicity of the whole submicron aerosol becomes obvious in Fig. 11. Compared with the threshold κ values for activation for S between 0.2 ~ 1.0 % (denoted by colored squares), most particles with D_{dry} larger than 150 nm can be activated for $S \geq 0.2$ % regardless of the choice of any measured κ value. On the other hand, the threshold κ for activation increases sharply with D_{dry} smaller than 100 nm and CCN activity becomes sensitive to κ. This method is denoted as "Method 2- GF (small)". A similar method of using a single κ for all sizes can be done with the average κ for the two largest diameters (200 and 250 nm), where aerosol mass faction is large. Various aerosol chemistry measurements like filter-based measurement or mass spectrometry rely on aerosol mass concentration. This method is denoted as "Method 2-GF (large)" and can be considered as a proxy for using such chemistry data for N_{CCN} closure.

Another way of assigning a single κ value is to use the κ values deduced from the S_c measurement. The S_c value for 50 nm was available only for less than half of Gosan 2008. Therefore the κ deduced from S_c for 100 nm was used as the single κ for N_{CCN} closure and this method is denoted as "Method 2-S_c".

In "Method 3-GF", the campaign-averaged κ values deduced from the GF measurements at the five different diameters shown in Table 3 are used to assign κ to each size

ACPD
11, 19683–19727, 2011

bin as explained in Fig. 10. Here the difference is that the temporal variation of κ during the campaign is ignored by using the campaign averages. "Method 3-S_c" is similar: the campaign-averaged κ value of 0.4 deduced from S_c for 100 nm (Table 3) is assigned for all size distribution data. Therefore, by comparing "Method 3" to "Method 1", the effect of temporal variation of hygroscopicity can be found.

For the last method, "Method 4", κ was set to 0.3 as suggested by AR08 and only the temporal variation of the size distribution was taken into account as in "Method 3".

The results of all closures are illustrated in Fig. 12 and the quantitative comparison of the results is made in Table 5 where the averages and standard deviations of relative deviation are shown, which is defined as the ratio of the absolute difference between the predicted and measured N_{CCN} to the measured N_{CCN}. The closure results only for the pollution days showed no noticeable difference (not shown) compared to those for non-pollution days.

For all methods, the smallest average relative deviation was found for 1.0 % S indicating that the importance of assigned κ information diminishes as S increases as most particles would be activated regardless of the κ value when S is high. The largest standard deviation of relative deviation was found for 0.6 % S, which means that the goodness of N_{CCN} prediction significantly varied from case to case for this S. For 0.6 % S, the measured κ was near the threshold value for 50 and 100 nm (Fig. 11) and therefore the predicted N_{CCN} was highly sensitive to the assigned κ.

Now we compare the different methods. It is found that the average κ for the two largest diameters (200 and 250 nm) poorly represents aerosol hygroscopicity for higher S: the relative deviation of "Method 2-GF (large)" for 0.6 % S is not only larger than "Method 2-GF (small)" but also larger than "Method 3-GF" where temporal variation of hygroscopicity was completely ignored. This suggests that chemistry information of aerosols smaller than 100 nm diameter cannot be substituted by bulk measurements that mostly represent aerosols of larger diameters than 100 nm. Kammermann et al. (2010) drew similar conclusion from their GF measurement that assigning the hygroscopicity measured for aerosols of diameter 180~200 nm to all size particles

ACPD
11, 19683–19727, 2011

resulted in poor CCN closure. Ervens et al. (2010) also made similar suggestion that identifying hydrophobic organics of diameter ~ 100 nm is important for CCN closure.

Because the relative deviation of Method 3-GF is comparable to that of Method 1-GF, it can be said that the effect of temporal variation of hygroscopicity had minor effect on CCN closure. However, it should be noted that Gosan 2008 lasted only 2 months and temporal variation of hygroscopicity may be important when one needs to deal with longer period.

The methods using the S_c data (Method 2-S_c, Method 3-S_c) show larger relative deviation than the methods using the GF data. Even the method using the constant κ (Method 4) shows smaller relative deviation. There were much more over-predicted than under-predicted values for these two methods (Fig. 12e and f), which is in accordance with Fig. 9b where κ (S_c) was larger than κ (GF) and mostly larger than $\kappa = 0.3$.

Figure 13 illustrates the detailed feature of over-prediction when $\kappa = 0.3$ (Method 4) was assumed at 0.6 % S. Here the relative deviations of Method 4 are compared to those of Method 1-GF as a function of N_{CCN}. The relative deviations of Method 4 tend to increase as N_{CCN} decreases from the largest ($3787 \sim 7203\,cm^{-3}$) to the smallest bin ($289 \sim 550\,cm^{-3}$) (Fig. 13a). There is a trend of increasing number fraction of particles with $D_{dry} < 100$ nm with the decrease of N_{CCN} (Fig. 13b). It is worth noting that although secondary particle formation and growth events occurred during Gosan 2008, the increasing relative deviations or number fraction of particles having $D_{dry} < 100$ nm cannot be attributed to these events since data during these events only took a minor fraction of the total data. Such correlated trends indicate that the over-prediction by Method 4 is due to assigning too high κ value for particles having $D_{dry} < 100$ nm (Fig. 11), which results in false activation of particles that are too small to be activated in reality. Kammermann et al. (2010) have found that the κ value of 0.3 predicts too large GF value which was rarely measured at subarctic site. It also explains why the method using GF data resulted in much less over-prediction and again demonstrates that hygroscopicity measurements for small aerosols ($D_{dry} < 100$ nm) are important for estimating N_{CCN}.

ACPD
11, 19683–19727, 2011

5 Summary and conclusion

Aerosol hygroscopicity, CCN spectra and critical supersaturation were measured at two remote islands (Gosan, Jeju Island and Baengnyeongdo Comprehensive Monitoring Observatory (BCMO), Baengnyeongdo) of Korea along with aerosol concentration and size distribution during four field campaigns held in: August 2006 (Gosan); April to May 2007 (Gosan); August to October 2008 (Gosan) and August 2009 (BCMO). CN concentrations (N_{CN}) at the two islands were comparable to the ones measured at the nearby seas, indicating that the local anthropogenic sources within the islands were negligible. However, $PM_{2.5}$, PM_{10}, SO_2, O_3 and CO concentrations measured at the two islands suggested that the two islands were constantly under anthropogenic influences from the Asian continent regardless of the season and year. Average values for all of the measured CCN concentration (N_{CCN}) at 0.2, 0.6 and 1.0 % supersaturations (S), N_{CN} and geometric mean diameter (D_g) from both islands were in the range of 1043–3051 cm^{-3}, 2076–4360 cm^{-3}, 2713–4694 cm^{-3}, 3890–5117 cm^{-3} and 81–98 nm, respectively, and BCMO recorded the highest N_{CCN} for all S when compared to the Gosan measurements. Significantly higher SO_2 concentration at BCMO may be responsible for the high N_{CCN}/N_{CN} for $S \leq 0.6$ % as SO_2 is the precursor of sulfates.

The aerosols were mostly internally mixed, although minor fraction of samples contained externally mixed hydrophobic aerosols. No significant differences in hygroscopicity were found between the pollution and non-pollution days at both islands suggesting that continental sources were constantly affecting the sites even on the days classified as non-pollution days. Larger hygroscopicity and lower S_c were measured at BCMO for all sizes than at Gosan, which is consistent with higher SO_2 concentration of BCMO. Generally, the hygroscopicity measured at the two islands was similar to that measured during ACE-Asia at the sea 500 km east of Gosan but was significantly higher than that measured at a downwind site of Beijing, indicating that aerosols measured at Gosan might have experienced aging processes during its transport to add hygroscopicity.

ACPD
11, 19683–19727, 2011

During the 2008 and 2009 campaigns, the critical supersaturation for cloud activation (S_c) of particles of selected sizes was estimated by the size-resolving N_{CCN}/N_{CN} measurement. The S_c at BCMO was distinctly different between the two periods when the air mass was from China (lower S_c) and from Korea/Japan (higher S_c) but such distinction was not observed at Gosan. By compiling all HTDMA and DMA-CCN measurements that have been conducted at Gosan since 2005, we suggest that aerosol hygroscopicity may have decreased for this period. To note is that the hygroscopicity estimated from the S_c measurements was higher than that from the GF measurements, the reason of which is not yet clear.

The temporally varying and size-resolving HTDMA hygroscopicity data successfully predicted N_{CCN} as the average relative deviation from the measured values was within 28 % for 0.2, 0.6 and 1.0 % S. Comparison of various CCN closure methods that used the HTDMA data suggested that it was crucial to know hygroscopicity of aerosols smaller than 100 nm diameter for predicting N_{CCN} accurately. Prescribing a fixed hygroscopicity value as suggested by Andreas and Rosenfeld (2008) for aged continental aerosols resulted in the average relative deviation in the range of 25–40 %. The relative deviation tended to increase with decreasing N_{CCN}, which was accompanied by increase of sub-100 nm fraction. Considering the fact that numerical models usually vary N_{CCN} to simulate the aerosol effects on clouds, such finding alludes to potential error of using a constant hygroscopicity as global representative value for aged continental aerosol.

Acknowledgements. The authors would like to express special thanks to Kim Prather of University of California, San Diego, for providing 2007 CN data. Special thanks also go to Mr. KyungSik Kang for providing all the local support during the 2006, 2007 and 2008 Gosan campaigns and to the staffs at BCMO for the 2009 BCMO campaign. This work was funded by the Korea Meteorological Administration Research and Development Program under Grant RACS_2010-5001.

ACPD
11, 19683–19727, 2011

References

Adhikari, M., Ishizaka, Y., Minda, H., Kazaoka, R., Jensen, J. B., Gras, G. L., and Nakajima, T.: Vertical distribution of cloud condensation nuclei concentrations and their effect on microphysical properties of clouds over the sea near the southwest islands of Japan, J. Geophys. Res., 110, D10203, doi:10.1029/2004JD004758, 2005.

Andreae, M. O. and Rosenfeld, D.: Aerosol–cloud–precipitation interactions – Part 1: The nature and sources of cloud-active aerosols, Earth-Sci. Rev., 89, 13–41, 2008.

Bates, T. S., Coffman, D. J., Covert, D. S., and Quinn, P. K.: Regional marine boundary layer aerosol size distributions in the Indian, Atlantic, and Pacific Oceans: a comparison of INDOEX measurements with ACE-1, ACE-2, and Aerosol 99, J. Geophys. Res., 107, D19, 8026, doi:10.1029/2001JD001174, 2002.

Brechtel, F. J. and Kreidenweis, S. M.: Predicting particle critical supersaturation from hygroscopic growth measurements in the humidified TDMA. Part I: Theory and sensitivity Studies, J. Atmos. Sci., 57, 1854–1871, 2000.

Covert, D. S., Kapustin, V. N., Bates, T. S., and Quinn, P. K.: Physical properties of marine boundary layer aerosol particles of the mid-Pacific in relation to sources and meteorological transport, J. Geophys. Res., 101, D3, 6919–6930, 1996.

Dusek, U., Covert, D. S., Wiedensohler, A., Neusüss, C., Weise, D., and Cantrell, W.: Cloud condensation nuclei spectra derived from size distributions and hygroscopic properties of the aerosol in coastal South-West Portugal during ACE-2, Tellus B, 55, 35–53, 2003.

Dusek, U., Frank, G. P., Hildebrandt, L., Curtius, J., Schneider, J., Walter, S., Chand, D., Drewnick, F., Hings, S., Jung, S., Borrmann, S., and Andreae, M. O.: Size matters more than chemistry for cloud-nucleating ability of aerosol particles, Science, 312, 1375–1378, 2006.

Eichler, H., Cheng, Y. F., Birmili, W., Nowak, A., Wiedensohler, A., Brüggemann, E., Gnauk, T., Herrmann, H., Althausen, D., Ansmann, A., Engelmann, R., Tesche, M., Wendisch, M., Zhang, Y. H., Hu, M., Liu, S., and Zeng, L. M.: Hygroscopic properties and extinction of aerosol particles at ambient relative humidity in South-Eastern China, Atmos. Environ., 42, 6321–6334, 2008.

Ervens, B., Cubison, M. J., Andrews, E., Feingold, G., Ogren, J. A., Jimenez, J. L., Quinn, P. K., Bates, T. S., Wang, J., Zhang, Q., Coe, H., Flynn, M., and Allan, J. D.: CCN predictions using simplified assumptions of organic aerosol composition and mixing state: a synthesis from

ACPD
11, 19683–19727, 2011

six different locations, Atmos. Chem. Phys., 10, 4795–4807, doi:10.5194/acp-10-4795-2010, 2010.
Flowers, B. A., Dubey, M. K., Mazzoleni, C., Stone, E. A., Schauer, J. J., Kim, S.-W., and Yoon, S. C.: Optical-chemical-microphysical relationships and closure studies for mixed carbonaceous aerosols observed at Jeju Island; 3-laser photoacoustic spectrometer, particle sizing, and filter analysis, Atmos. Chem. Phys., 10, 10387–10398, doi:10.5194/acp-10-10387-2010, 2010.
Gasparini, R., Collins, D. R., Andrews, E., Sheridan, P. J., Ogren, J. A., and Hudson, J. G.: Coupling aerosol size distributions and size-resolved hygroscopicity to predict humidity-dependent optical properties and cloud condensation nuclei spectra, J. Geophys. Res., 111, D05S13, doi:10.1029/2005JD006092, 2006.
Gunthe, S. S., King, S. M., Rose, D., Chen, Q., Roldin, P., Farmer, D. K., Jimenez, J. L., Artaxo, P., Andreae, M. O., Martin, S. T., and Pöschl, U.: Cloud condensation nuclei in pristine tropical rainforest air of Amazonia: size-resolved measurements and modeling of atmospheric aerosol composition and CCN activity, Atmos. Chem. Phys., 9, 7551–7575, doi:10.5194/acp-9-7551-2009, 2009.
Hobbs, P. V.: Introduction to Atmospheric Chemistry, 276 pp., Cambridge University Press, 2000.
Hoppel, W. A., Fitzgerald, W., Frick, G. M., and Larson, R. E.: Aerosol size distributions and optical properties found in the marine boundary layer over the Atlantic Ocean, J. Geophys. Res., 95, D4, 3659–3686, 1990.
Hudson, J. G.: An instantaneous CCN spectrometer, J. Atmos. Ocean. Tech., 1055–1065, 1989.
Hudson, J. G.: Variability of the relationship between particle size and cloud-nucleating ability, Geophys. Res. Lett., 34, L08801, doi:10.1029/2006GL028850, 2007.
Hudson, J. G. and Da, X.: Volatility and size of cloud condensation nuclei, J. Geophys. Res., 101, D2, 4435–4442, 1996.
Huebert, B. J., Bates, T., Russell, P. B., Shi, G., Kim, Y. J., Kawamura, K., Carmichael, G., and Nakajima, T.: An overview of ACE-Asia: Strategies for quantifying the relationships between Asian aerosols and their climatic impacts, J. Geophys. Res., 108, D23, 8633, doi:10.1029/2003JD003550, 2003.
IPCC: Climate Change 2007: The physical science basis. Contribution of Working Group I to the Fourth Assessment Report of the Intergovernmental Panel on Climate Change, edited

ACPD
11, 19683–19727, 2011

by: Solomon, S., Qin, D., Manning, M., Chen, Z., Marquis, M., Averyt, K. B., Tignor, M., and Miller, H. L., Cambridge University Press, 2007.
Kammermann, L., Gysel, M., Weingartner, E., Herich, H., Cziczo, D. J., Holst, T., Svenningsson, B., Arneth, A., and Baltensperger, U.: Subarctic atmospheric aerosol composition: 3. Measured and modeled properties of cloud condensation nuclei, J. Geophys. Res., 115, D04202, doi:10.1029/2009JD012447, 2010.
Kaneyasu, N.: Long-term measurement of aerosols on a remote island in the Northwest Pacific Ocean, International Aerosol Conference 2010, Helsinki, Finland, International Aerosol Research Assembly, 2010.
Khain, A., Ovtchinnikov, M., Pinsky, M., Pokrovsky, A., and Krugliak, H.: Notes on the state-of-the-art numerical modeling of cloud microphysics, Atmos. Res., 55, 159–224, 2000.
Kim, J. H., Yum, S. S., Lee, Y.-G., and Choi, B.-C.: Ship measurements of submicron aerosol size distributions over the Yellow Sea and the East China Sea, Atmos. Res., 93, 700–714, 2009a.
Kim, S. K., Kong, B. J., Park, J. S., Lee, S. D., Kim, J. S., Lee, S. J.: The characteristic of particle composition at Baengnyeong Island, Technical report of National Institute of Environmental Research, NO. 2009-45-1101, 2009b (in Korean with English abstract).
Kim, S.-W., Yoon, S-C., Jefferson, A., Ogren, J. A., Dutton, E. G., Won, J.-G., Ghim, Y. S., Lee, B.-I., Han J.-S.: Aerosol optical, chemical and physical properties at Gosan, Korea during Asian dust and pollution episodes in 2001, Atmos. Environ., 39, 39–50, 2005.
Knutson, E. O. and Whitby, K. T.: Aerosol classification by electric mobility: Apparatus, theory, and applications, J. Aerosol. Sci., 6, 443–451, 1975.
Kumala, M., Vehkamäki, H. Petäjä, T., Dal Maso, M., Lauri, A., Kerminen, V.-M., Birmili, W., and McMurry, P. H.: Formation and growth rates of ultrafine atmospheric particles: a review of observations, J. Aerosol Sci., 35, 143–176, 2004.
Kuwata, M. and Kondo, Y.: Dependence of size-resolved CCN spectra on the mixing state of nonvolatile cores observed in Tokyo, J. Geophys. Res., 113, D19202, doi:10.1029/2007JD009761, 2008.
Kuwata, M., Kondo, Y., Miyazaki, Y., Komazaki, Y., Kim, J. H., Yum, S. S., Tanimoto, H., and Matsueda, H.: Cloud condensation nuclei activity at Jeju Island, Korea in spring 2005, Atmos. Chem. Phys., 8, 2933–2948, doi:10.5194/acp-8-2933-2008, 2008.
Lance, S., Nenes, A., Mazzoleni, C., Dubey, M. K., Gates, H., Varutbangkul, V., Rissman, T. A., Murphy, S. M., Sorooshian, A., Flagan, R. C., Seinfeld, J. H., Feingold, G., and Jons-

ACPD
11, 19683–19727, 2011

son, H. H.: Cloud condensation nuclei activity, closure, and droplet growth kinetics of Houston aerosol during the Gulf of Mexico Atmospheric Composition and Climate Study (GoMACCS), J. Geophys. Res., 114, D00F15, doi:10.1029/2008JD011699, 2009.

Lee, M., Song, M., Moon, K. J., Han, J. S., Lee, G., and Kim, K.-R.: Origins and chemical characteristics of fine aerosols during the Northeastern Asia regional experiment (Atmospheric Brown Cloud–East Asia Regional Experiment 2005), J. Geophys. Res., 112, D22S29, doi:10.1029/2006JD008210, 2007.

Massling, A., Leinert, S., Wiedensohler, A., and Covert, D.: Hygroscopic growth of submicrometer and one-micrometer aerosol particles measured during ACE-Asia, Atmos. Chem. Phys., 7, 3249–3259, doi:10.5194/acp-7-3249-2007, 2007.

Massling, A., Stock, M., Wehner, B., Wu, Z. J., Hu, M., Brüggemann, E., Gnauk, T., Herrmann, H., and Wiedensohler, A.: Size segregated water uptake of the urban submicrometer aerosol in Beijing, Atmos. Environ., 43, 1578–1589, 2009.

Matsumoto, K., Tanaka, H., Nagao, I., and Ishizaka, Y.: Contribution of particulate sulfate and organic carbon to cloud condensation nuclei in the marine atmosphere, Geophys. Res. Lett., 24, 665–658, 1997.

Mochida, M., Nishita-Hara, C., Kitamori, Y., Aggarwal, S. G., Kawamura, K., Miura, K., and Takami, A.: Size-segregated measurements of cloud condensation nucleus activity and hygroscopic growth for aerosols at Cape Hedo, Japan, in spring 2008, J. Geophys. Res., 115, D21207, doi:10.1029/2009JD013216, 2010.

Nakajima, T., Yoon, S.-C., Ramanathan, V., Shi, G.-Y., Takemura, T., Higurashi, A., Takamura, T., Aoiki, K., Sohn, B.-J., Kim, S.-W., Tsuruta, H., Sugimoto, N., Shimizu, A., Tanimoto, H., Sawa, Y., Lin, N.-H., Lee, C.-T., Goto, D., and Schutgens, N.: Overview of the Atmospheric Brown Cloud East Asian Regional Experiment 2005 and a study of the aerosol direct radiative forcing in East Asia, J. Geophys. Res., 112, D24S91, doi:10.1029/2007JD009009, 2007.

Petters, M. D. and Kreidenweis, S. M.: A single parameter representation of hygroscopic growth and cloud condensation nucleus activity, Atmos. Chem. Phys., 7, 1961–1971, doi:10.5194/acp-7-1961-2007, 2007.

Petters, M. D. and Kreidenweis, S. M.: A single parameter representation of hygroscopic growth and cloud condensation nucleus activity – Part 2: Including solubility, Atmos. Chem. Phys., 8, 6273–6279, doi:10.5194/acp-8-6273-2008, 2008.

Pruppacher, H. R. and Klett, J. D.: Microphysics of Clouds and Precipitation, 954 pp., Springer,

ACPD
11, 19683–19727, 2011

New York, 1997.
Ramana, M. V., Ramanathan, V., Feng, Y., Yoon, S.-C., Kim, S.-W., Carmichael, G. R., and Schauer, J. J.: Warming influenced by the ratio of black carbon to sulphate and the black-carbon source, Nat. Geosci., 3, 542–545, doi:10.1038/ngeo918, 2010.
Roberts, G. C. and Nenes, A.: A continuous-flow streamwise thermal-gradient CCN chamber for atmospheric measurements, Aerosol Sci. Tech., 39, 206–221, 2005.
Rose, D., Gunthe, S. S., Mikhailov, E., Frank, G. P., Dusek, U., Andreae, M. O., and Pöschl, U.: Calibration and measurement uncertainties of a continuous-flow cloud condensation nuclei counter (DMT-CCNC): CCN activation of ammonium sulfate and sodium chloride aerosol particles in theory and experiment, Atmos. Chem. Phys., 8, 1153–1179, doi:10.5194/acp-8-1153-2008, 2008.
Rose, D., Nowak, A., Achtert, P., Wiedensohler, A., Hu, M., Shao, M., Zhang, Y., Andreae, M. O., and Pöschl, U.: Cloud condensation nuclei in polluted air and biomass burning smoke near the mega-city Guangzhou, China – Part 1: Size-resolved measurements and implications for the modeling of aerosol particle hygroscopicity and CCN activity, Atmos. Chem. Phys., 10, 3365–3383, doi:10.5194/acp-10-3365-2010, 2010.
Schwartz, S. E., Charlson, R. J., Khan, R. A., Ogren, J. A., Rodhe, H.: Why Hasn't Earth Warmed as Much as Expected?, J. Climate, 23, 2453–2464, 2010.
Stith, J. L., Ramanathan, V., Cooper, W. A., Roberts, G. C., DeMott, P. J., Carmichael, G., Hatch, C. D., Adhikary, B., Twohy, C. H., Rogers, D. C., Baumgardner, D., Prenni, A. J., Campos, T., Gao, R., Anderson, J., and Feng, Y.: An overview of aircraft observations from the Pacific Dust Experiment campaign, J. Geophys. Res., 114, D05207, doi:10.1029/2008JD010924, 2009.
Su, H., Rose, D., Cheng, Y. F., Gunthe, S. S., Massling, A., Stock, M., Wiedensohler, A., Andreae, M. O., and Pöschl, U.: Hygroscopicity distribution concept for measurement data analysis and modeling of aerosol particle mixing state with regard to hygroscopic growth and CCN activation, Atmos. Chem. Phys., 10, 7489–7503, doi:10.5194/acp-10-7489-2010, 2010.
Swietlicki, E., Zhou, J., Berg, O. H., Martinsson, B. G., Frank, G., Cederfelt, S.-I., Dusek, U., Berner, A., Birmili, W., Wiedensohler, A., Yuskiewicz, B., and Bower, K. N.: A closure study of sub-micrometer aerosol particle hygroscopic behavior, Atmos. Res., 50, 205–240, 1999.
Swietlicki, E., Hansson, H.-C., Hämeri, K., Svenningsson, B., Massling, A., McFiggans, G., McMurry, P. H., Petäjä, T., Tunved, P., Gysel, M., Topping, D., Wiengartner, E., Baltensperger, U.,

ACPD
11, 19683–19727, 2011

Rissler, J., Wiedensohler, A., and Kulmala, M.: Hygroscopic properties of submicrometer atmospheric aerosol particles measured with H-TDMA instruments in various environments – a review, Tellus B, 60, 432–469, 2008.

Vestin, A., Rissler, J., Swietlicki, E., Frank, G. P., and Andreae, M. O.: Cloud-nucleating properties of the Amazonian biomass burning aerosol: cloud condensation nuclei measurements and modeling, J. Geophys. Res., 112, D14201, doi:10.1029/2006JD008104, 2007.

Wang, J., Cubison, M. J., Aiken, A. C., Jimenez, J. L., and Collins, D. R.: The importance of aerosol mixing state and size-resolved composition on CCN concentration and the variation of the importance with atmospheric aging of aerosols, Atmos. Chem. Phys., 10, 7267–7283, doi:10.5194/acp-10-7267-2010, 2010.

Wex, H., McFiggans, G., Henning, S., and Stratmann, F.: Influence of the external mixing state of atmospheric aerosol on derived CCN number concentrations, Geophys. Res. Lett., 37, L10805, doi:10.1029/2010GL043337, 2010.

Wiedensohler, A., Cheng, Y. F., Nowak, A., Wehner, B., Achtert, P., Berghof, M., Birmili, W., Wu, Z. J., Hu, M., Zhu, T., Takegawa, N., Kita, K., Kondo, Y., Lou, S. R., Hofzumahaus, A., Holland, F., Wahner, A., Gunthe, S. S. Rose, D., Su, H., and Pöschl, U.: Rapid aerosol particle growth and increase of cloud condensation nucleus activity by secondary aerosol formation and condensation: A case study for regional air pollution in Northeastern China, J. Geophys. Res., 114, D00G08, doi:10.1029/2008JD010884, 2009.

Yum, S. S. and Hudson, J. G.: Vertical distributions of cloud condensation nuclei spectra over the springtime Arctic Ocean, J. Geophys. Res., 106, D14, 15045–15052, 2001.

Yum, S. S., Hudson, J. G., Song, K. Y., and Choi, B.-C.: Springtime cloud condensation nuclei concentrations on the west coast of Korea, Geophys. Res. Lett., 32, L09814, doi:10.1029/2005GL022641, 2005.

Yum. S. S., Roberts, G., Kim, J. H., Song, K., and Kim, D.: Submicron aerosol size distributions and cloud condensation nuclei concentrations measured at Gosan, Korea, during the Atmospheric Brown Clouds-East Asian Regional Experiment 2005, J. Geophys. Res., 112, D22S32, doi:10.1029/2006JD008212, 2007.

Zhou, J., Swietlicki, E., Hansson, H. C., and Artaxo, P.: Submicrometer aerosol particle size distribution and hygroscopic growth measured in the Amazon rain forest during the wet season, J. Geophys. Res., 107, D20, 8055, doi:10.1029/2000JD000203, 2002.

ACPD
11, 19683–19727, 2011

Table 1. Average and standard deviation of N_{CN}, N_{CCN}, N_{CCN}/N_{CN}, and D_g for each campaign.

Location (Year) Period		Gosan (2006) 15 Aug–1 Sep	Gosan (2007) 14 Apr–16 May	Gosan (2008) 1 Aug–11 Oct	BCMO (2009) 5–30 Aug
N_{CN} (cm^{-3})		4697 ± 1823	4217 ± 1514	3890 ± 1808	5117 ± 1880
N_{CCN} (cm^{-3})	1.0 % S	3290 ± 1964	4074 ± 1857[1]	2713 ± 1271	4694 ± 2567
	0.6 % S	2803 ± 1545	3527 ± 1718[1]	2076 ± 989	4360 ± 2297[2]
	0.2 % S	1550 ± 659	1952 ± 1286[1]	1043 ± 646	3051 ± 1310
N_{CCN}/N_{CN}	1.0 % S	0.77 ± 0.16	0.96 ± 0.15[1]	0.83 ± 0.31	0.87 ± 0.14
	0.6 % S	0.67 ± 0.12	0.81 ± 0.15[1]	0.60 ± 0.25	0.82 ± 0.16[2]
	0.2 % S	0.40 ± 0.06	0.44 ± 0.14[1]	0.29 ± 0.15	0.59 ± 0.20
D_g (nm)		98 ± 25	94 ± 14	81 ± 24[3]	94 ± 8[4]

[1] Only for the period between 20 April and 4 May.
[2] N_{CCN} and N_{CCN}/N_{CN} for 0.59 % S.
[3] The sample was dried prior to the measurement.
[4] Only for the period between 26 and 28 August.

ACPD
11, 19683–19727, 2011

Table 2. Average and standard deviation of GF90 and cumulative number fraction (NF) of each hygroscopicity class; class 1, 2, 3 and 4 corresponds to "nearly hydrophobic", "less hygroscopic", "more hygroscopic" and "very hygroscopic", respectively.

Period	D_{dry} (nm)	GF90_1	GF90_2	GF90_3	GF90_4	NF_1	NF_2	NF_3	NF_4
Gosan 2006	50	1.00±0.06	1.40±0.11	1.59±0.03	–	0.29±0.31	0.61±0.32	0.10±0.19	–
	100	1.05±0.04	1.50±0.05	1.66±0.06	–	0.22±0.23	0.33±0.38	0.45±0.33	–
	150	1.04±0.03	1.52±0.02	1.71±0.09	1.87±0.03	0.14±0.22	0.22±0.37	0.59±0/40	0.05±0.16
	200	1.02±0.02	1.51±0.03	1.67±0.08	1.87±0.02	0.10±0.15	0.15±0.21	0.66±0.30	0.09±0.16
	250	–	–	–	–	–	–	–	–
Gosan 2007	50	–	–	–	–	–	–	–	–
	100	1.07±0.04	1.48±0.06	1.58±0.03	–	0.05±0.08	0.66±0.23	0.30±0.25	–
	150	1.05±0.03	1.48±0.05	1.57±0.01	–	0.05±0.11	0.70±0.26	0.25±0.24	–
	200	1.04±0.05	1.47±0.04	1.57±0.01	2.17*	0.03±0.10	0.67±0.25	0.30±0.25	0.04*
	250	1.08±0.04	1.48±0.05	1.58±0.02	–	0.03±0.06	0.66±0.25	0.32±0.23	–
Gosan 2008	50	1.07±0.04	1.32±0.07	–	–	0.22±0.25	0.78±0.25	–	–
	100	1.08±0.05	1.32±0.06	–	–	0.14±0.25	0.86±0.25	–	–
	150	1.06±0.04	1.41±0.06	1.57±0.01	–	0.09±0.19	0.87±0.22	0.05±0.14	–
	200	1.08±0.02	1.43±0.05	1.58±0.02	–	0.04±0.10	0.88±0.23	0.09±0.21	–
	250	1.06±0.02	1.44±0.04	1.57±0.01	–	0.03±0.10	0.85±0.25	0.12±0.24	–
BCMO 2009	53	1.07±0.03	1.47±0.08	1.65±0.04	–	0.04±0.08	0.24±0.31	0.72±0.31	–
	113	0.99±0.02	1.50±0.04	1.62±0.04	–	0.01±0.03	0.25±0.32	0.74±0.32	–
	163	1.06±0.02	1.42±0.16	1.74±0.06	1.87±0.03	0.01±0.04	0.04±0.11	0.87±0.20	0.09±0.19
	225	1.08±0.07	1.51±0.04	1.68±0.06	1.92±0.05	0.04±0.10	0.07±0.15	0.85±0.21	0.04±0.13

* Only a single measurement was available.

ACPD
11, 19683–19727, 2011

Table 3. Comparison of κ values obtained from various hygroscopicity studies in East Asia. In BCMO 2009 and Massling et al. (2007), the results were classified by air mass back trajectories (nC: Northern China, KP: Korean Peninsula, KJ: Korea/Japan, Sd: Shanghai/dust). The measured values in column 3 are understood to be $D_{p\_act}(S_c)$ for DMA-CCN (D_{dry} scan), GF(D_{dry}) for HTMDA and $S_c(D_{dry})$ for DMA-CCN(S scan).

Location (Period)	Method	$D_{p\_act}(S_c)$, GF(D_{dry}) or $S_c(D_{dry})$	κ	Reference
Gosan, south of Korean Peninsula (Mar–Apr 2005)	DMA-CCN (D_{dry} scan)	136 ± 17 nm (0.097 %)* 71 ± 6 nm (0.27 %)* 44 ± 3 nm (0.58 %)* 31 ± 3 nm (0.97 %)*	0.61 ± 0.17* 0.55 ± 0.12* 0.50 ± 0.09* 0.55 ± 0.13*	Kuwata et al. (2008)
Gosan, south of Korean Peninsula (Aug 2006)	HTDMA	1.33 ± 0.15 (50 nm) 1.49 ± 0.14 (100 nm) 1.55 ± 0.19 (150 nm) 1.61 ± 0.14 (200 nm)	0.28 ± 0.15 0.41 ± 0.14 0.49 ± 0.18 0.53 ± 0.16	This study
Gosan, south of Korean Peninsula (Apr–May 2007)	HTDMA	1.48 ± 0.07 (100 nm) 1.48 ± 0.05 (150 nm) 1.48 ± 0.05 (200 nm) 1.49 ± 0.06 (250 nm)	0.25 ± 0.04 0.23 ± 0.03 0.23 ± 0.04 0.23 ± 0.05	This study
Gosan, south of Korean Peninsula (Aug–Oct 2008)	HTDMA	1.30 ± 0.08 (50 nm) 1.31 ± 0.06 (100 nm) 1.41 ± 0.06 (150 nm) 1.43 ± 0.06 (200 nm) 1.45 ± 0.05 (250 nm)	0.17 ± 0.05 0.16 ± 0.04 0.21 ± 0.04 0.22 ± 0.05 0.23 ± 0.04	This study
	DMA-CCN (S scan)	0.19 ± 0.02 % (100 nm)	0.40 ± 0.07	This study
BCMO, west of Korean Peninsula (Aug 2009)	HTDMA**	1.61 ± 0.06 (53 nm, nC) 1.60 ± 0.06 (113 nm, nC) 1.74 ± 0.06 (163 nm, nC) 1.67 ± 0.06 (225 nm, nC)	0.42 ± 0.05 0.36 ± 0.04 0.48 ± 0.05 0.41 ± 0.04	This study

ACPD
11, 19683–19727, 2011

Table 3. Continued.

Location (Period)	Method	$D_{p\_act}(S_c)$, GF(D_{dry}) or $S_c(D_{dry})$	κ	Reference
	DMA-CCN (S scan)	0.33 ± 0.08 % (81 nm, KP) 0.22 ± 0.04 % (110 nm, KP) 0.22 ± 0.02 % (81 nm, nC) 0.15 ± 0.01 % (110 nm, nC)	0.28 ± 0.12 0.35 ± 0.09 0.52 ± 0.07 0.43 ± 0.05	This study
East Sea (Apr 2001)	HTDMA	1.55 (50 nm, KJ)*** 1.69 (150 nm, KJ)*** 1.67 (250 nm, KJ)*** 1.64 (350 nm, KJ)*** 1.62 (50 nm, Sd)*** 1.68 (150 nm, Sd)*** 1.61 (250 nm, Sd)*** 1.54 (350 nm, Sd)***	0.35 *** 0.44 *** 0.42 *** 0.39 *** 0.41 *** 0.43 *** 0.36 *** 0.30 ***	Massling et al. (2007)
Cape Hedo, Japan (Apr 2007)	HTDMA	1.39 ± 0.06 (49 nm)[1] 1.43 ± 0.05 (71 nm)[1] 1.47 ± 0.04 (125 nm)[1]	0.37 ± 0.07[1] 0.39 ± 0.05[1] 0.42 ± 0.04[1]	Mochida et al. (2010)
	DMA-CCN (D_{dry} scan)	130 ± 3 nm (0.10 %) 78 ± 5 nm (0.25 %) 54 ± 5 nm (0.44 %)	0.69[2] 0.51[2] 0.50[2]	Mochida et al. (2010)
Beijing, Northeastern China (Jun–Jul 2004)	HTDMA	1.23 (50 nm)*** 1.37 (150 nm)*** 1.42 (250 nm)*** 1.45 (350 nm)***	0.11*** 0.18*** 0.21*** 0.23***	Massling et al. (2009)
Beijing, Northeastern China (Jan–Feb 2005)	HTDMA	1.27 (50 nm)*** 1.36 (150 nm)*** 1.30 (250 nm)*** 1.28 (350 nm)***	0.14*** 0.18*** 0.14*** 0.12***	Massling et al. (2009)
Yufa, Northeastern China (23 Aug 2006)	DMA-CCN (D_{dry} scan)	190 ± 3 nm (0.07 %) 84 ± 5 nm (0.26 %) 62 ± 6 nm (0.46 %) 45 ± 7 nm (0.86 %)	0.45[3] 0.38[3] 0.30[3] 0.22[3]	Wiedensohler et al. (2009)

* Taken from Table 2 of Kuwata et al. (2008).
** No HTDMA results were available for KP back trajectories.
*** Average GF were calculated from number-weight averaging of the GF values measured at 90 % RH in each hygroscopicity class given in the appendix tables in each study. Corresponding κ values were then calculated from the average GF90 with $T = 15\,^{\circ}C$.
[1] GF values were measured at 85 % RH. Taken from Table 2 of Mochida et al. (2010).
[2] Calculated from average D_{p_act} in Table 1 of Mochida et al. (2010) with $T = 15\,^{\circ}C$.
[3] Calculated from average D_{p_act} in Fig. 12 of Wiedensohler et al. (2009) with $T = 15\,^{\circ}C$.

ACPD
11, 19683–19727, 2011

Table 4. Parameters C and k of the power law approximation of the CCN spectra based on the measured CCN spectra for the S range of 0.2–1.0 % ($S \geq 0.2$ %) and those for the S range of 0.02–0.2 % ($S \leq 0.2$ %) in each campaign.

Period	$S \geq 0.2$ %	$S \leq 0.2$ %
Gosan 2006	(3438 cm^{-3}, 0.47)	(8977 cm^{-3}, 1.04)
Gosan 2007	(4194 cm^{-3}, 0.32)	N/A
Gosan 2008	(2533 cm^{-3}, 0.41)	(9012 cm^{-3}, 1.32)
BCMO 2009	(4879 cm^{-3}, 0.28)	(36304 cm^{-3}, 1.60)

ACPD
11, 19683–19727, 2011

Table 5. Average and standard deviation of relative deviation, defined as $|N_{CCN\_pred} - N_{CCN\_meas}|/N_{CCN\_meas}$, for different CCN closure methods using the GF and S_c data. The values are given in the units of percent.

Method	1-GF	2-GF (small)	2- GF (large)	3-GF	2-S_c	3-S_c	4
0.2 % S	28 ± 20	32 ± 17	25 ± 24	28 ± 38	38 ± 42	50 ± 68	30 ± 51
0.6 % S	25 ± 52	25 ± 51	31 ± 57	26 ± 39	42 ± 57	47 ± 61	41 ± 56
1.0 % S	19 ± 15	19 ± 14	22 ± 17	23 ± 29	30 ± 37	34 ± 42	28 ± 35

ACPD
11, 19683–19727, 2011

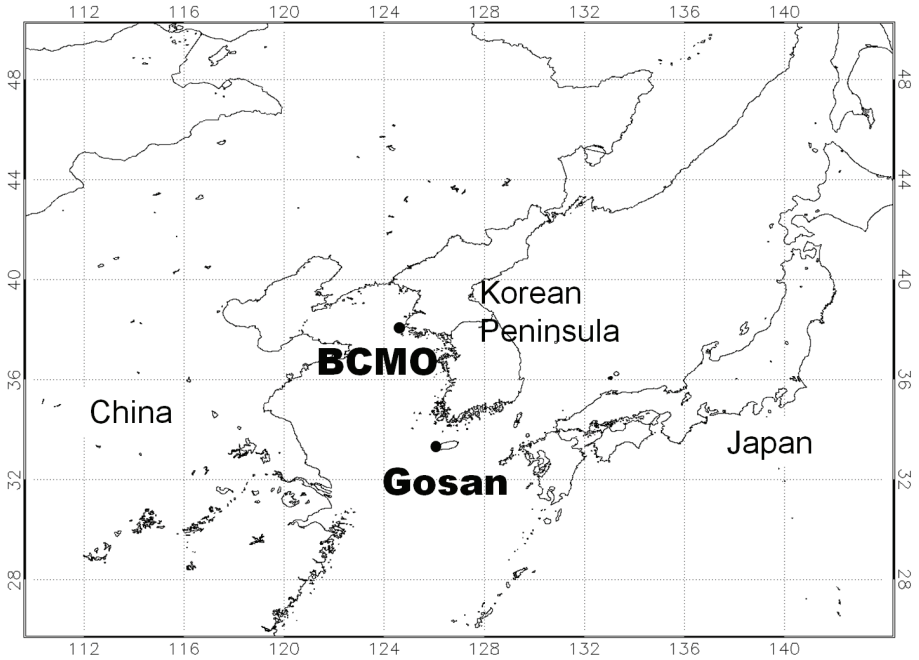

Fig. 1. Locations of the measurement sites, Gosan and BCMO (Baengnyeongdo Comprehensive Monitoring Observatory).

ACPD
11, 19683–19727, 2011

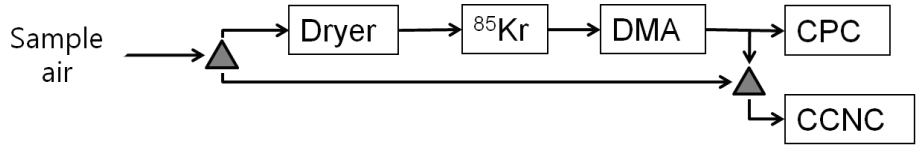

Fig. 2. Configuration of instruments for measuring N_{CCN} and characterizing S_c during Gosan 2008 and BCMO 2009.

ACPD
11, 19683–19727, 2011

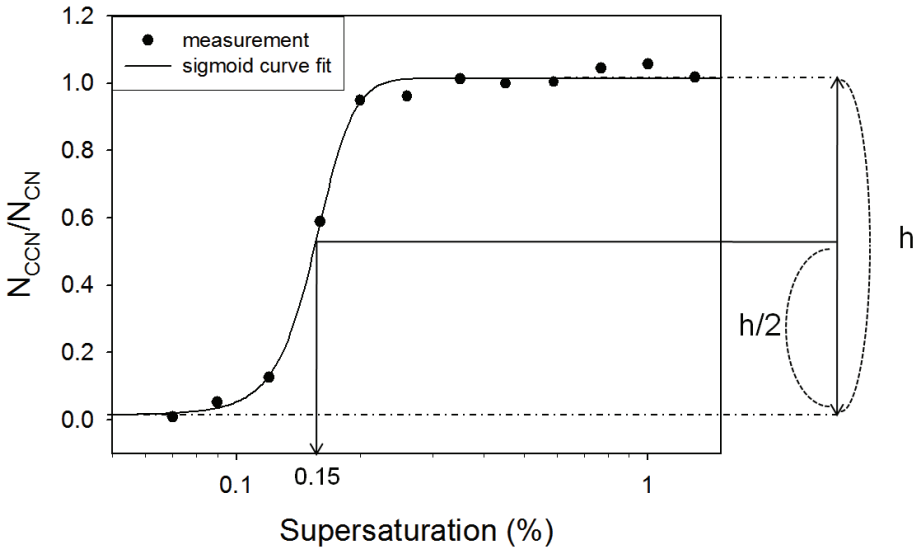

Fig. 3. Example of S_c characterization for dry particle of 110 nm.

ACPD
11, 19683–19727, 2011

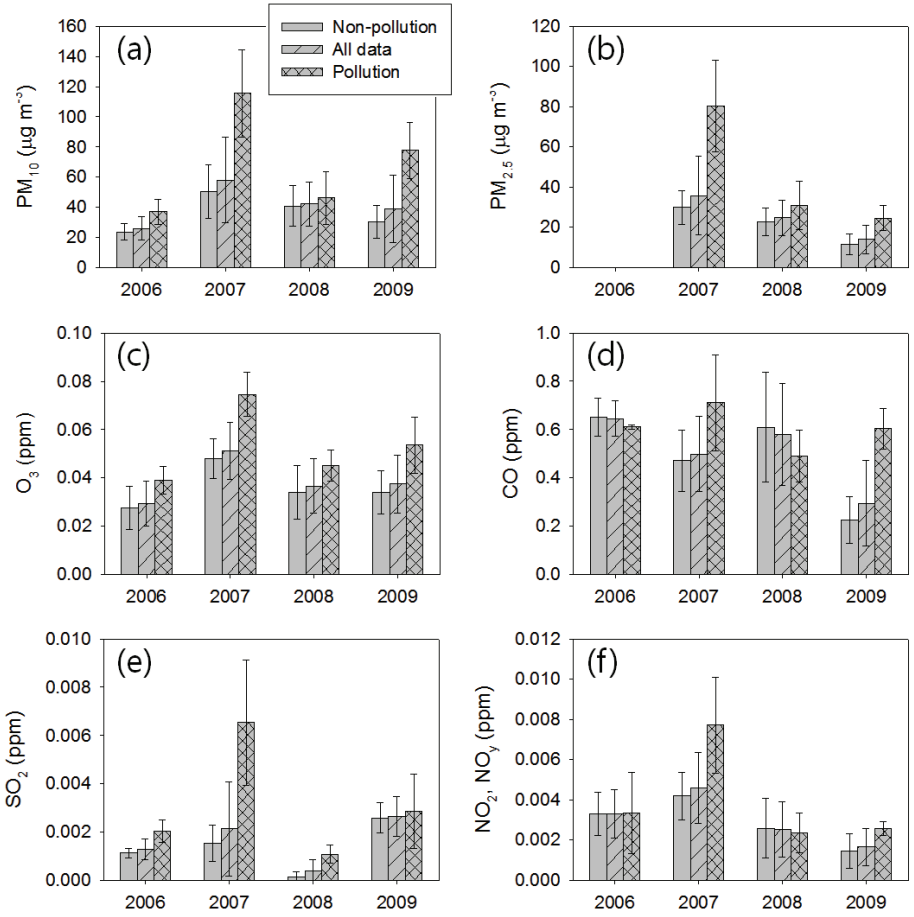

Fig. 4. Average values of PM mass concentrations and various gaseous species for each campaign.

ACPD
11, 19683–19727, 2011

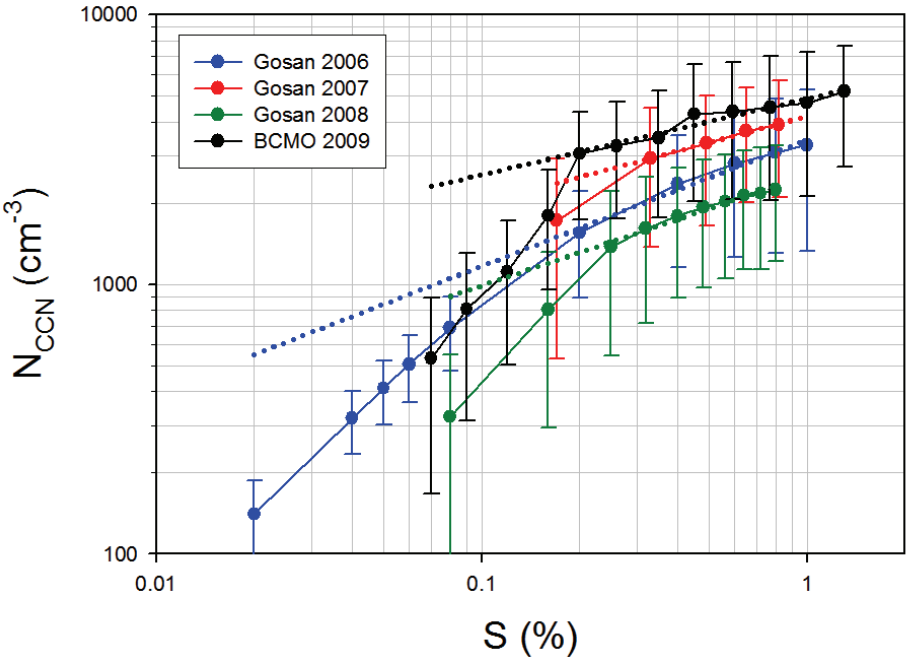

Fig. 5. Average CCN spectra (solid line) and power-law approximation for $S \geq 0.02\,\%$ (dotted line).

ACPD
11, 19683–19727, 2011

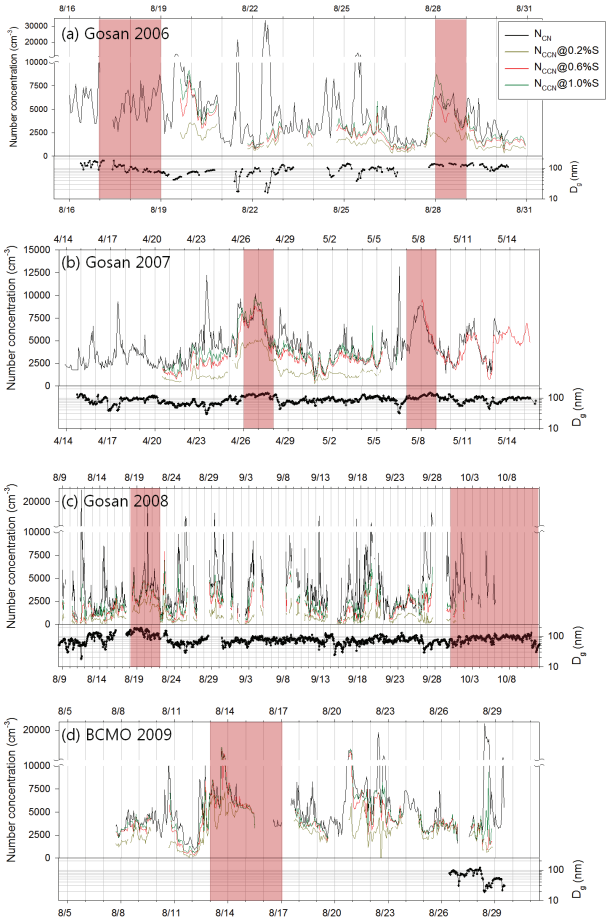

Fig. 6. Time plots of measured N_{CN}, N_{CCN} and D_g for each campaign. Pollution periods are shaded in red.

ACPD
11, 19683–19727, 2011

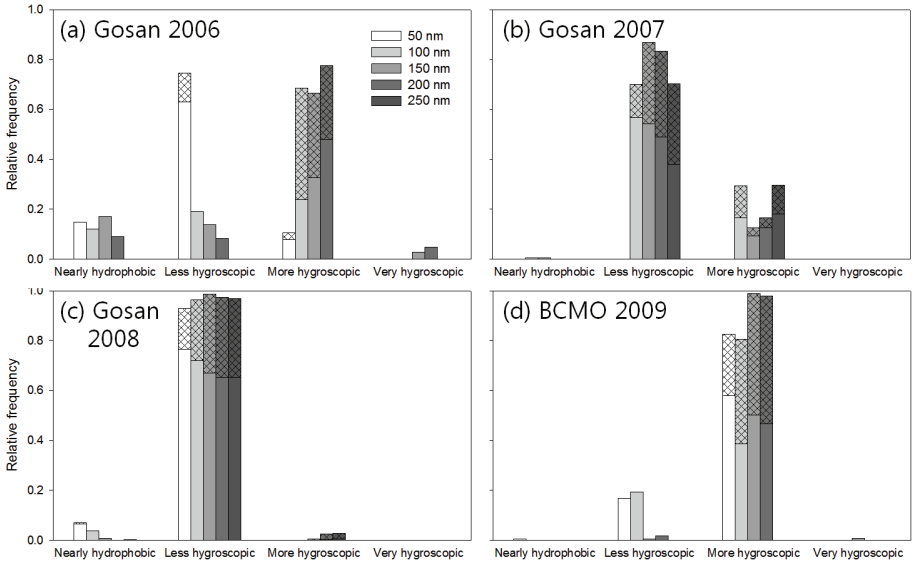

Fig. 7. Relative frequency of occurrence of each hygroscopicity class for each dry diameter during each campaign. Meshed part indicates the portion for pollution days. For BCMO 2009, dry diameters are 53, 113, 163, 225 nm.

ACPD
11, 19683–19727, 2011

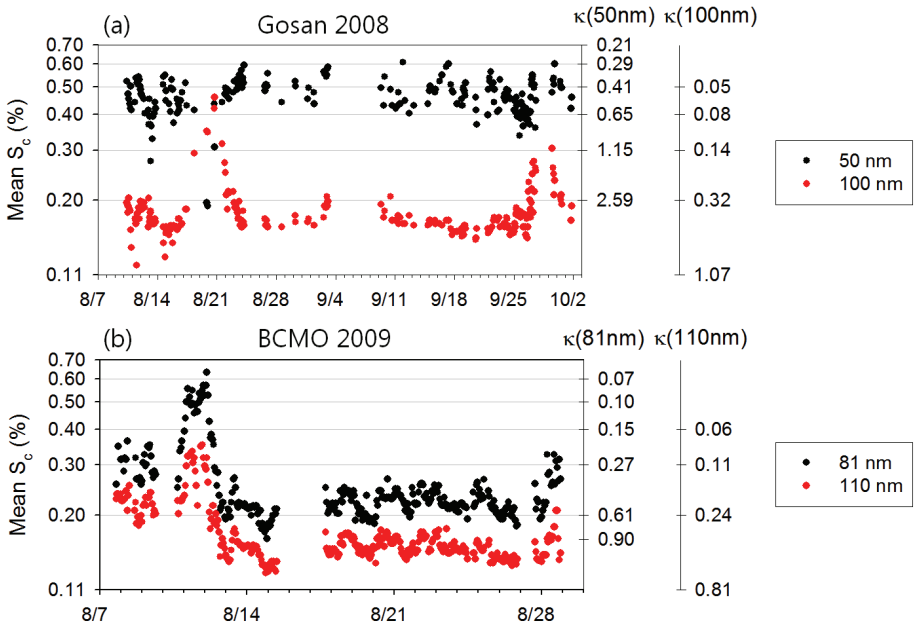

Fig. 8. Time plots of S_c during Gosan 2008 (top) and BCMO 2009 (bottom). The κ values for corresponding S_c values for each dry diameter are shown on the right.

ACPD
11, 19683–19727, 2011

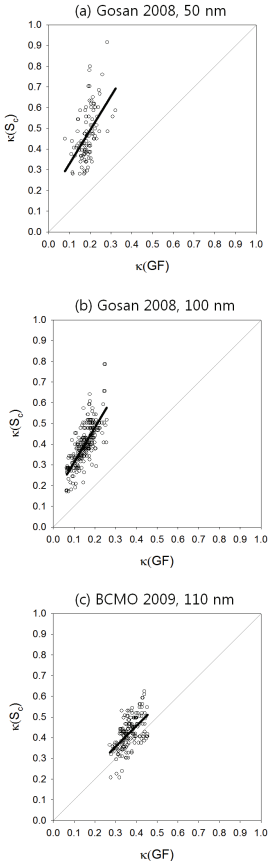

Fig. 9. Comparison of the estimated κ values from GF and S_c measurements for 50 and 100 nm D_{dry} during Gosan 2008 and for 110 nm D_{dry} during BCMO 2009. The linear regression lines are shown as thick solid line.

ACPD
11, 19683–19727, 2011

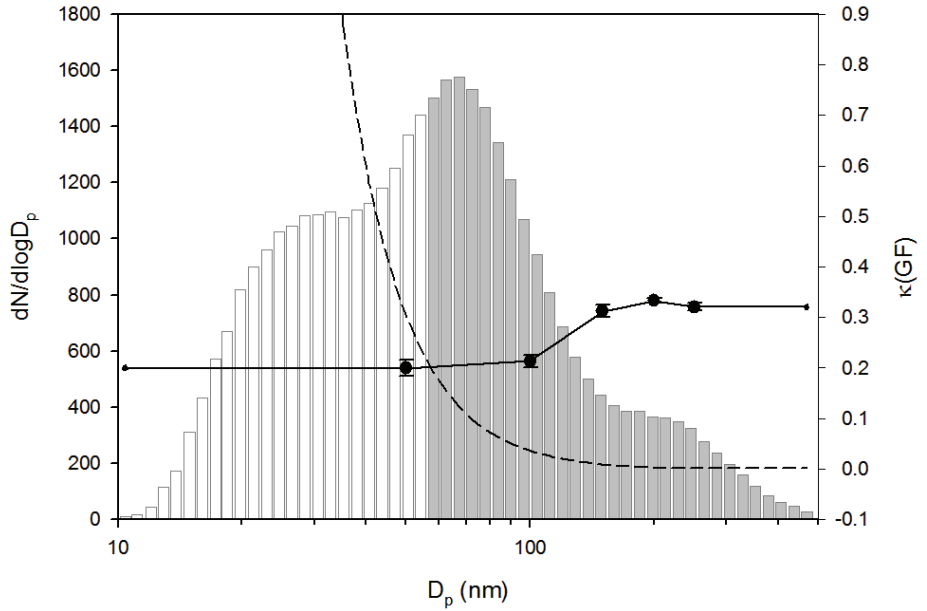

Fig. 10. An example of predicting N_{CCN} at 0.6 % S by combining measured κ (GF) (line with circle symbols) with the size distribution. The dashed line denotes the minimum κ required for each size bin to be activated as CCN at 0.6 % S. Only the grey vertical boxes are summed up to obtain the predicted N_{CCN} based on the GF measurement.

ACPD
11, 19683–19727, 2011

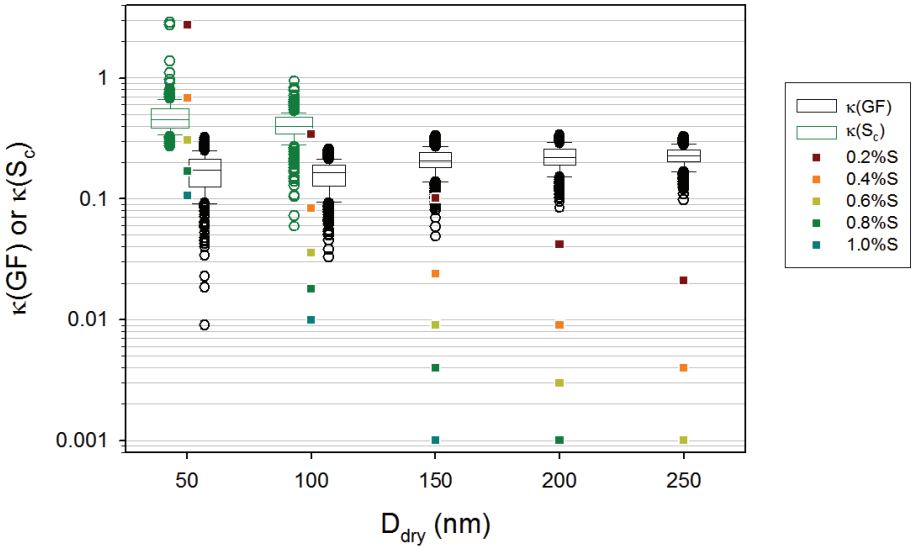

Fig. 11. Hygroscopicity parameter κ for each D_{dry} during Gosan 2008. Threshold κ values for cloud activation under selected S are shown as colored squares.

ACPD
11, 19683–19727, 2011

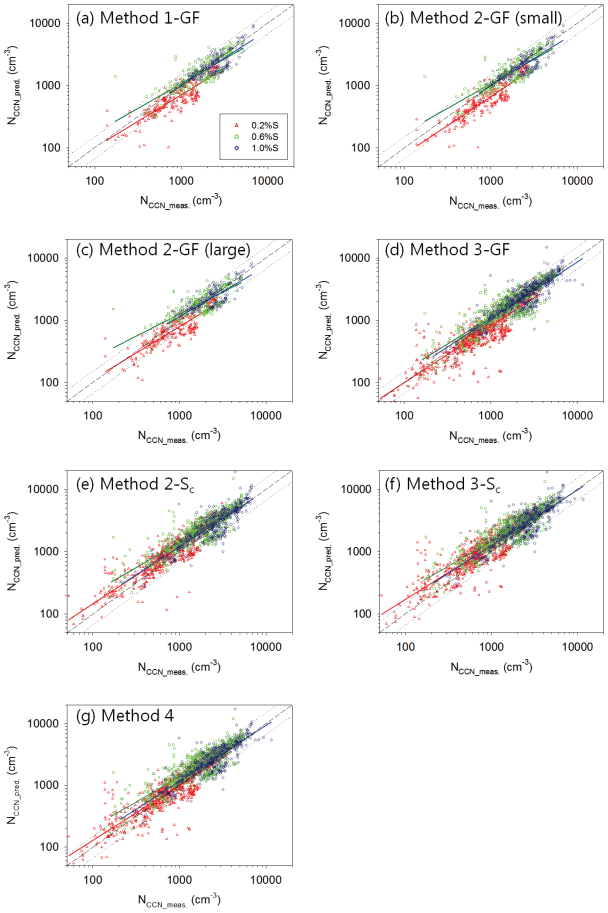

Fig. 12. CCN closure results from various methods. For the description of each method, see the text. The dotted lines indicate ±50 % error.

ACPD
11, 19683–19727, 2011

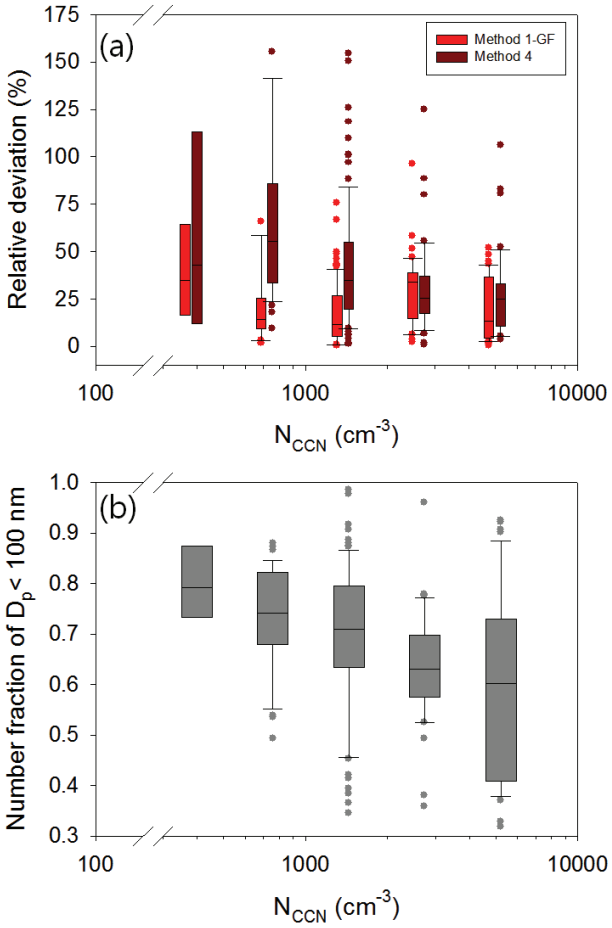

Fig. 13. (a) Relative deviations, defined as $|N_{CCN\_pred}–N_{CCN\_meas}|/N_{CCN}$, for methods 1 and 4, and **(b)** the number fraction of particles smaller than 100 nm D_p for each N_{CCN} bins.

ACPD
11, 19683–19727, 2011